DRFC/CAD

EUR-CEA-FC-1641

One-Dimensional Full Wave Treatment of Mode Conversion Process at the Ion-Ion Hybrid Resonance in a Bounded Tokamak Plasma

I. Monakhov, A. Bécoulet, D. Fraboulet, F. NGuyen

Septembre 1998

One-dimensional full wave treatment of mode conversion process at the ion-ion hybrid resonance in a bounded tokamak plasma

I. Monakhov[a)], A. Bécoulet, D. Fraboulet, F. Nguyen

Association EURATOM-CEA sur la Fusion Contrôlée,

Centre d'Etudes de Cadarache, 13108 Saint-Paul-lez-Durance, France

ABSTRACT

A consistent picture of the mode conversion (MC) process at the ion-ion hybrid resonance in a bounded plasma of a tokamak is discussed, which clarifies the role of the global fast wave interference and cavity effects in the determination of the MC efficiency. This picture is supported by simulations with one-dimensional full wave kinetic code "VICE". The concept of the "global resonator", formed by the $R=n_{||}^2$ boundary cut-offs [B. Saoutic *et al.*, Phys. Rev. Lett. **76**, 1647 (1996)], is justified, as well as the importance of a proper tunneling factor choice $\eta_{cr}=0.22$ [A. K. Ram *et al.*, Phys. Plasmas **3**, 1976 (1996)]. The MC scheme behavior appears to be very sensitive to the MC layer position relative to the global wave field pattern, i.e. to the local value of "poloidal" electric field at the resonance. Optimal MC regimes are found to be attainable without requirement of a particular parallel wavenumber choice.

PACS '98 CODES: 52.55Fa, 52.50Gj, 52.25Sw, 52.65Tt

[a)] Permanent address : Troitsk Institute of Innovative and Thermonuclear Investigations, Troitsk, Moscow region 142092 Russia

I. INTRODUCTION

Tokamak plasma heating and current drive methods, based on external excitation of radio waves in the ion cyclotron range of frequencies (ICRF) are characterized by a large variety of experimental scenarios[1], which are considered to be quite perspective for application in future tokamak-reactor. Last years significant interest in ICRF investigations was drawn to a scheme using the mode conversion (MC) phenomena near the ion-ion hybrid resonance in conditions where the fast magnetosonic wave (FW) is launched from the low field side (LFS) of the tokamak and relative concentrations of the ion species are chosen to be roughly equal, in order to locate the ion cyclotron resonances far away from the MC layer. This approach seems to have good possibilities to solve several important reactor-relevant problems, such as electron temperature and current profile control[2], channeling of the alpha-particles energy to fuel ions[3] and low-hybrid current drive efficiency enhancement[4,5]. The reliability of the scheme was successfully verified during experiments on several large-scale tokamaks[6,7,8]; simultaneously some theoretical studies were undertaken[5,9,10,11] to justify the discussed scenario because its suitability was not quite obvious until recently.

In this paper, an attempt is made to demonstrate a consistent one-dimensional (1D) picture of the mode conversion process in a bounded plasma of a tokamak. Qualitative model, based on simple cold plasma considerations and supported by computer simulations with a one-dimensional full wave kinetic code, is presented. The influence of the global fast wave interference and cavity effects on the MC efficiency is clarified, and the role of competitive FW damping mechanisms is

discussed. Along with its generalizing meaning, this treatment is valuable in a sense that it provides guidelines for optimal experimental parameters definition and evaluates the capabilities of the MC electron heating scheme.

In Sec. II, a brief review is given, concerning the current status of the mode conversion problem, and the necessity of a more systematic MC treatment in a bounded plasma is justified. In Sec. III, a typical mode conversion picture, produced by full wave kinetic code simulations, is examined and principal features of the code are discussed. In Sec. IV, peculiarities of the mode conversion phenomena in bounded plasma of a tokamak are analyzed in details: first, a behavior of the global field pattern as predicted by simple cold plasma model and computed by 1D simulations is qualitatively discussed. Then, an approach to adequate quantitative MC characterization in a bounded 1D plasma is proposed. Parameters are defined, which are used further in numerical studies of the MC efficiency. Basic features of cavity effects are also investigated here. Finally, some practical consequences of the studies are mentioned and the relevance of 1D model to the real situation is discussed. Sec. V contains a summary of the treatment.

II. STATUS OF THE PROBLEM

An importance of the mode conversion phenomena for rf wave propagation and absorption in plasma was recognized long time ago[12] and a possibility to use it for laboratory plasma heating was discussed since early stages of thermonuclear activities[13]. In cold plasma approximation, the MC process manifests itself in unlimited growth of rf field amplitude near the region where the value of the perpendicular wavenumber, given by the local dispersion relation, turns to infinity. To

make the problem physically meaningful some artificial mechanism, removing the singularity, needs to be introduced in this model, thus allowing the computation of the power absorbed at the resonance. When thermal effects are taken into account the nature of this mechanism becomes clear, because the singularity is resolved by the occurrence of a short-scale warm plasma wave, extracting the energy from the incident wave in the vicinity of the resonant region. Near the ion-ion hybrid resonance the fast magnetosonic wave is mode converted to a short quasipotential mode, known as the ion Bernstein wave (IBW)[14] , whose wavelength is of the order of the ion Larmor radius.

Among the numerous peculiarities of IBW behavior in a tokamak plasma[15,16], beyond the scope of this article, one is worth mentioning here, namely the fact, that IBW can efficiently transfer its energy to electrons by Landau damping mechanism, providing there is no ion (bulk or impurity) cyclotron layers along its ray trajectory. It is worthwhile also to note that, due to a strong variation of the parallel wavenumber $k_{||}$ along the ray trajectory, the mode-converted IBW is inevitably damped somewhere in plasma. Thus leaving aside the question of the power deposition profiles, we only address the central problems of the MC scheme: what is the total amount of rf power which can be converted from FW to IBW, and what are the best conditions to achieve this maximum? In the tokamak plasma with density and magnetic field gradients, the problem turns to be rather complicated even in a simple 1D geometry. Indeed, an analysis of the FW perpendicular refractive index behavior

$$n_{\perp}^2 = \frac{(L-n_{||}^2)(R-n_{||}^2)}{(S-n_{||}^2)} = \frac{(S-n_{||}^2)^2 - D^2}{(S-n_{||}^2)} \qquad (1)$$

shows, that the MC resonance $S=n_{||}^2$ is typically accompanied very close on its low

field side by the FW cut-off $L=n_{||}^2$ layer. This cut-off-resonance pair is surrounded in turn by the boundary cut-offs $R=n_{||}^2$. (The cold plasma model neglecting the electron mass is discussed here; Stix notations[13] are used for the coordinate system orientation and the dielectric tensor elements S=(L+R)/2 and D=(R-L)/2). Two principal features of the mode conversion in a tokamak plasma are then envisioned: 1) the asymmetry relative to the location of FW launching (high field side (HFS) versus LFS), due to the internal cut-off, and 2) the susceptibility to interference and cavity effects, due to the FW reflections on the boundary cut-offs.

At the beginning of MC studies in a tokamak plasma, the effect of asymmetry was considered to be dominant and the main efforts were directed to investigate phenomena in the vicinity of an isolated cut-off-resonance pair, the incoming and outgoing FWs being treated as asymptotic solutions of an appropriate differential equation, describing the wave fields near the resonance[17,18,19]. The basic conclusions of this approach are clear from the Budden equation analysis

$$\frac{d^2E_y}{dx^2}+\frac{\omega^2}{c^2}Q(x)E_y=0, \tag{2}$$

where the "potential" function Q(x) coincides with the right-hand side of the cold plasma dispersion relation (see Eqn.(1)). After linearization of S and D elements near the x=0 resonance $S=n_{||}^2$ point, the equation can be written as

$$\frac{d^2E_y}{dx^2}+k_{\perp\infty}^2(1-\frac{\Delta}{x})E_y=0, \tag{3}$$

where $k_{\perp\infty}^2 = -\frac{2\omega^2 D D'}{c^2 S'}$ is the asymptotic (far away from the resonance) FW perpendicular wavenumber and $\Delta = -\frac{D}{2D'}$ is the internal evanescent layer thickness, i.e. the distance between the $S=n_{||}^2$ resonance and the $L=n_{||}^2$ cut-off (Here primes denote differentiation with respect to x and the tensor elements are evaluated at x=0). Resorting to the familiar technique of the singularity elimination ($x \rightarrow x+i\varepsilon$, where $\varepsilon \rightarrow +0$) and integrating the expression of the radial Pointing flux gradient

$$\frac{dF_x}{dx} = \frac{1}{2\mu_0\omega} \mathrm{Im}(E_y^* \frac{d^2E_y}{dx^2}) \tag{4}$$

over the resonance region, one can find (e.g. see Ref. 20) an instructive expression for the power, absorbed in the MC region (the mode converted power) :

$$P_{mc} = \frac{\pi}{2}\varepsilon_0\omega\frac{D^2}{S'}\left|E_y^{mc}\right|^2 = \frac{\pi}{2\mu_0\omega}k_{\perp\infty}\eta\left|E_y^{mc}\right|^2, \tag{5}$$

where $\eta=k_{\perp\infty}\Delta$ is the so-called tunneling parameter and $|E_y^{mc}|$ is the local value of the "poloidal" electric field at the $S=n_{||}^2$ resonance.

When an isolated cut-off-resonance pair is treated, the $|E_y^{mc}|$ field amplitude is decreased, as compared to the amplitude of the falling wave, due to the FW evanescence in between the internal cut-off and the $S=n_{||}^2$ resonance. As this evanescence depends also on η, the tunneling parameter is recognized in Budden approach as the only factor determining the MC efficiency (This conclusion was verified in more sophisticated models[21], accounting for finite electron mass and temperature effects). The fraction T of power of the incident FW, which is transmitted

through the cut-off-resonance doublet, appears to be independent on the FW excitation direction and equal to:

$$T=\exp(-\pi\eta). \tag{6}$$

The remaining fraction is totally mode-converted without any reflection in the case of a high field side (HFS) FW excitation, and is partitioned between the reflected power fraction

$$R=(1-\exp(-\pi\eta))^2=(1-T)^2 \tag{7}$$

and the mode converted power fraction

$$C=\exp(-\pi\eta)(1-\exp(-\pi\eta))=T(1-T) \tag{8}$$

in the case of the LFS excitation. It is clear that, in the latter case, the mode converted power fraction reaches its maximum value of C=0.25 for T=0.5 conditions, which correspond to a critical value of the tunneling parameter

$$\eta_{cr}=\frac{\ln(2)}{\pi}\cong 0.22 \quad . \tag{9}$$

Since Δ is increasing linearly with the tokamak major radius and $k_{\perp\infty}$ is rising with plasma density, this initial analysis gave the practical conclusion that the MC scheme in large-scale tokamaks can only be efficient under conditions of HFS FW launching. The results of experiments with HFS antennas seemed to support this picture[22]. The role of the ion-ion hybrid resonance during the LFS FW excitation was considered to be important only in the sense that it significantly enhances the amplitude of the left-hand polarized component of the rf electric field in the vicinity of the cyclotron layer of minority ions, thus increasing their cyclotron acceleration[23].

The previous judgments can be disputed when the problem is treated in a bounded plasma, where the local value of $|E_y^{mc}|$ depends not only on the internal evanescence of the incident FW as discussed hereabove, but also on its interference with the reflected waves. In accordance with Eqn.(1), the MC efficiency should be very sensitive to the $S=n_{||}^2$ resonance location relative to the global E_y pattern, as built by the FW reflections in the plasma cavity. The first attempts to evaluate the role of the HFS boundary $R=n_{||}^2$ cut-off in the MC process were made in the framework of the Alfvén resonance analyses[13,20,24]. An influence of interference between incoming and reflected FW on the mode conversion at the second ion-cyclotron harmonic was reported also[25]. Some years ago, the importance of this interference phenomena in ion-ion hybrid resonance MC scheme was recognised[2]. A model was proposed[5,9,10], which treats cut-off-resonance-cut-off triplet, formed by the usual Budden pair and the HFS $R=n_{||}^2$ cut-off layer, as an internal plasma resonator. The mode conversion enhancement was identified as the critical coupling between the incident FW and this resonator, in a situation where certain phase relations are fulfilled. It was shown that, in optimal conditions of T=0.5 (which are the same as for an isolated Budden pair), up to 100% of incoming FW power can be mode converted, and that the only factor lowering this value is a competitive direct FW damping.

The proposed picture gave serious background to successful MC experiments with LFS antennas, but at the same time it left some problems unclear. It was found, that both conditions of optimal triplet resonator phasing and its optimal coupling to the FW (T=0.5) are dependent on the tunneling parameter η. Thus, for a given value of

plasma density, a careful HFS $R=n_{||}^2$ cut-off layer position matching is necessary, and should be done by an appropriate choice of the launched FW parallel wavenumber. This leads to the questionable conclusion, that good MC conditions could be achieved only for a narrow $k_{||}$ range, which may not coincide with the maximum of the antenna radiated spectrum. Another drawback of this model comes from the fact, that it treats only the part of the FW interference pattern, which is formed on the HFS of the MC layer by the wave incoming from and outgoing to a LFS infinity. In real situation, this pattern is a result of multiple FW reflections from both HFS and LFS boundary $R=n_{||}^2$ cut-off layers, as well as from the internal $L=n_{||}^2$ cut-off layer. Moreover, according to Budden considerations there is no power reflection for the wave falling on the MC layer from the HFS of the tokamak, so the region between the HFS $R=n_{||}^2$ and $L=n_{||}^2$ cut-offs could never be treated as a resonator in full sense; thus, no cavity mode effects can take place in this triplet structure, being treated separately.

The importance of cavity effects was evidently demonstrated experimentally and numerically during MC activities on Tore Supra[7]. The proposed approach relies on the reasonable idea that the FW, bouncing in the "global resonator" structure, formed by $R=n_{||}^2$ cut-offs, is inevitably mode converted, providing other damping mechanisms are weak. The latter assumption implies a careful analysis of all the possible damping mechanisms. If the direct FW electron Landau damping (ELD) and transit time magnetic pumping (TTMP) competitive mechanisms are well understood[9,11] and can be considered quite weak (at least for present day tokamaks), the role of ion cyclotron (IC) absorption in the MC scheme is not clear yet. Indeed, the

IC damping can be completely avoided only by placing the cyclotron layers of both ion species outside the plasma. This can be achieved practically only in tokamaks with large R_0/a aspect ratio and for ion mixture with roughly equal concentrations. But in this conditions, the tunneling parameter η is maximized which, as will be clear later, can be unfavorable for the MC heating scheme. The total shift of the IC layer of light ions (low Z/A ratio) out of the plasma on the LFS is also undesirable because it leads to additional cut-off-resonance pair appearance in the LFS plasma periphery regions in front of the antenna[18], with possible deleterious edge heating effects. Besides, the IC layer can cross the antenna structure elements, which may cause electrical breakdowns. Thus, the most realistic version of the MC scheme apparently should be based on moderate relative ion concentrations with the light ion cyclotron layer being located in the LFS plasma regions, somewhere near the half of its minor radius. In such conditions the ion-cyclotron damping does not look negligible *a priori* and its competitive role needs to be taken into account.

It is quite clear that the most adequate description of the MC phenomena in a bounded plasma can be given by the full-wave computer modeling. A number of codes has been developed and applied to MC studies in 1D geometry[26-32]. The simulations have shown that the wave reflections and cavity effects are of the primary importance for the MC process. These phenomena can manifest themselves as a sharp increase of the antenna radiation resistance[28] and of the power absorbed in MC layer vicinity. The mode conversion coefficient at certain conditions appeared to be much higher, than it was predicted by Budden treatment[27,29], recovering its "classical" values only in the case where the boundary reflections were artificially suppressed[29]. At the same time,

this simulations did not provide a coherent picture about the limiting factors and optimum conditions for the MC scheme. Also the relation of full-wave computational results with previously discussed analytical models was not clarified.

III. FULL WAVE MODELLING AND COMPUTER CODE SPECIFICATION

In the next section, an attempt is made to give a more systematic picture of MC phenomena under conditions of the LFS FW excitation. Qualitative considerations are supported by simulations with the one-dimensional full-wave computer code "VICE"("Variational Ion Cyclotron Emission"). The code was created for studying the problems of ion-cyclotron emission in a tokamak plasma[32,33] and is capable of self-consistent treatment of particles interaction with ICRF waves of arbitrary scale and polarization. The code solves the linearized Maxwell-Vlasov system of equations for bounded current-less multispecies plasma in a plane geometry. The general approach, used in "VICE" is the same as was utilized first for the development of the 2D full wave "ALCYON" code[34,35]. The unperturbed particle trajectories, as well as the various wave-particle interactions, are treated using the Hamiltonian formalism in the action-angle variable space with the vector and scalar potentials being used for the wave field description. Neglecting exact particles trajectories, relevant for 2D tokamak geometry, the "VICE" code has certain advantages, which are especially important for adequate MC treatment : 1) unlike "ALCYON", which considers only the fast wave, "VICE" consistently takes into account all the components of the potentials, thus making possible to analyze the waves of arbitrary polarization; 2) the mesh size can be made small enough (less than 1mm for Tore Supra parameters, examined later) to resolve small-scale hot plasma modes, such as IBWs; 3) higher order terms with

respect to the ion Larmor radius are retained in the Hamiltonian (up to the third order for the present version of the code), which leads to more correct cyclotron damping calculations. It is worthwhile to note also, that the Hamiltonian approach allows to avoid the definition of the local wave vector, which in situations like the present one can be questionable. Thus, the "VICE" code is an appropriate tool, suitable for studying MC phenomena in a hot bounded plasma with accompanying effects of IBW and FW damping due to IC, ELD and TTMP mechanisms, FW reflections and 1D cavity mode formation. The general formalism, numerical procedures, results of the code verification and a comparison with WKB solutions are discussed in details in Ref. 33.

With the intention to use simulations not only for illustrative purpose but having in mind the generality of the MC picture, the following plasma parameters, relevant for Tore Supra[36] tokamak, were used in computations: R_0=2.37 m, a=0.75 m, B_0=3.8 T, H+^{3}He ion mixture, $T_e(0)$=1.5 keV, $T_i(0)$=1.0 keV, $n_e(0)$=3-8×10^{19} m^{-3}. Unlike the previous analysis[7], based on the avoidance of any competitive damping mechanisms, here we tried to investigate more complicated situation, where the ion cyclotron damping is not necessarily negligible. Thus, smaller relative hydrogen-to-helium concentration ratio was used (n_H/n_{He}=0.4) and the frequency range of f=50-60 MHz was studied in order to place the MC layer near the plasma center. In such conditions, the fundamental cyclotron harmonic layer of hydrogen is located only about 14 cm on the LFS of the MC layer, crossing the central hot plasma regions. At the same time, this distance is not sufficiently small for the "minority ion heating" scenario to be dominant and the general features of the MC scheme remain valid. For clarity, all results presented here were produced for the single toroidal harmonic of the

antenna current spectrum ($k_{||}=14\ m^{-1}=33/R_0$), corresponding to the maximum of the Tore Supra dipole phased antenna spectrum. Simple parabolic and squared parabolic radial profiles were chosen respectively for plasma density and temperature description, with $n(a)=0.1 \cdot n(0)$ edge density pedestal and an exponential decay within a region of a±0.1m (decay length λ=3cm). An infinitely thin antenna sheet was located at a+0.03m position. Plasma parameters were supposed to be varied in direction of the "radial" x-axis, the antenna current directed along the "poloidal" y-axis and the vector of "toroidal" magnetic field inductance directed along the z-axis.

The typical picture of the MC process, produced by "VICE" for the specified plasma parameters and f=54MHz, $n_e(0)=4\times10^{19}\ m^{-3}$ is shown on Fig.1 together with the hot plasma dispersion curves (Fig.1(a)). At the FW-IBW confluence point the rf electric field amplitudes are increasing sharply, whereas in the bulk plasma volume (between the boundary cut-offs) they form a standing fast wave pattern. The logarithmic representation of the field amplitudes and absorbed powers is used in order to demonstrate the relative role of the various damping mechanisms. The electron power deposition profile correlates clearly with the parallel electric field amplitude distribution; the power deposition is very peaked near the MC layer, which can be seen also from the radial Pointing flux behavior (by the MC layer we understand the confluence point of FW and IBW branches, given by the hot plasma dispersion relation). It is important to note, that the electron power deposition in the MC layer is about two orders of magnitude higher than the FW ELD and TTMP damping in the rest of the plasma volume. This gives us the ground to consider further all power, absorbed by electrons as being the mode-converted power. The calculated profile of the power density p_H, absorbed by hydrogen ions, follows the behavior of

the left-hand polarized component of the perpendicular electric field $|E_+|$. It is clear from the figure, that in spite of some $|E_+|$ amplification near the MC layer, the total p_H increase in this region is small. It is worthwhile to mention also that the ion cyclotron absorption zone is quite wide because of large value of the parallel wavenumber. That is why the integral power, delivered to hydrogen, is not very sensitive to the local value of electric field at the location of $\omega=\omega_{cH}$ layer. As for the integral electron power deposition, which characterizes the MC efficiency, the situation is quite opposite. It was found that the MC layer exact location relative to the nodes and antinodes of the standing wave pattern is of paramount importance, determining the FW damping rate and the total power equipartition. This observations form the core of the present analysis and will be detailed further.

IV. MODE CONVERSION IN A BOUNDED PLASMA

A. Peculiarities of the global field pattern

In accordance with Budden considerations (see Eqn.(5)), the starting points of MC studies in a bounded plasma are certainly: 1) the determining role of the local "poloidal" electric field $|E_y^{mc}|$ at the MC layer and 2) the strong dependence of the global field pattern configuration on the tunneling factor η.

Relying on the concept of the global plasma resonator[7], let us at first qualitatively discuss a global picture of MC process in a bounded plasma. For the sake of clarity, we assume that all competitive damping mechanisms are negligible and that the MC region (internal evanescence and power deposition zone) is narrow as compared to the FW wavelength and the plasma minor radius. The first assumption

will be released in computer simulations and the second is justified for all situations of practical interest. In such an approach, the global field pattern can always be conceived as an interference of incoming and outgoing fast waves (The former are defined here as the waves going towards the HFS regions, and the latter as going towards the LFS regions). Simple analysis shows that the MC layer divides whole plasma into two parts with different behavior of the field patterns. In the high field side regions the pattern is formed as an interference of two waves with equal amplitudes: the incoming FW, transmitted through the cut-off-resonance pair and the FW, reflected from the HFS $R=n_{||}^2$ cut-off. Thus, the HFS pattern always has a nature of purely standing wave for any value of η and arbitrary resonance position. In the LFS region the FW, incoming from the antenna, interferes with two outgoing waves : one is transmitted from the HFS of the resonance and another is reflected on $L=n_{||}^2$ cut-off. The amplitudes of these backward going waves depend on η in opposite manner, being equal at $\eta=\eta_{cr}$ (see Eqs. (6), (7) and (8)). Their phase difference is sensitive to the resonance position; as a result, the LFS interference pattern depends both on the tunneling parameter and on the MC layer location. When $\eta=\eta_{cr}$ and the MC layer position coincides with the antinode of the global $|E_y|$ field pattern, the phases of outgoing waves are opposite[37] in LFS region and the waves cancel each other. The LFS wave pattern is thus represented solely by the incident FW, traveling from the antenna. Conversely, when the MC layer coincides with the global field node and P_{mc} is negligible (Eqn.(5)), the backward going waves have the same phases and the sum of their amplitudes is equal to the amplitude of the incident FW; accordingly, the LFS pattern (as well as the entire pattern) has a purely standing wave nature.

These peculiarities of the global field pattern were clearly revealed during "VICE" full wave simulations. The frequency variation was chosen for scanning the MC layer in the radial direction. This scan did not affect the tunneling parameter, as it was independently controlled by a plasma density adjustment: η_{cr}=0.22 corresponds to $n_e(0) \cong 4\times10^{19} m^{-3}$. Figure 2 shows the typical radial behavior of the "poloidal" electric field amplitude $|E_y|$ for various positions of the MC layer in conditions of $\eta \cong \eta_{cr}$. It can be seen that the global field pattern is not strongly distorted by the presence of the internal evanescence zone. The pattern in the HFS region always has a nature of a standing wave, whereas in the LFS region the traveling wave component appears as the MC layer moves closer to the global pattern antinode. At f=55MHz, the $|E_y|$ field pattern in the LFS region exhibits an almost pure traveling wave structure ($|E_y^{max}| \cong |E_y^{min}|$).

Previous considerations about the role of MC layer location relative to the global field pattern generally remain true for arbitrary value of the tunneling parameter, although some additional features should be mentioned. As the backward going fast waves for $\eta \neq \eta_{cr}$ always have different amplitudes in LFS region, the standing wave component never vanishes here, being minimal when the MC layer coincides with the global antinode. Besides, with increasing η value, the field structure turns to be significantly distorted by a strong local FW evanescence near the MC resonance and for $\eta >> \eta_{cr}$ a global node always follows the MC layer. This can be seen on Fig.3, where the global $|E_y|$ field patterns are shown for various values of the tunneling parameter (various plasma densities); the frequency being matched near f=55MHz for each η value to fit the maximum MC conditions (i.e. maximize $|E_y^{mc}|$).

It is clear from Fig.3 that the LFS traveling wave component has maximum at $\eta=\eta_{cr}$ and reasonable values of $|E_y^{mc}|$ are achievable only in conditions of $\eta<1$.

B. Mode conversion characterization in one-dimensional bounded plasma

Before going further, some remarks should be made concerning the phenomenon description. It is clear that any attempt to give quantitative picture of the MC process in a bounded plasma immediately faces the problem that traditional description in terms of T and R power fractions is no more suitable. Indeed, all rf power radiated by an antenna in a closed space should be damped somewhere, making the concept of transmitted and reflected powers meaningless. Some information about the MC process can be given by the antenna radiation resistance[28] or the absolute absorbed power[7] dependence studies, the latter being preferable because it allows to evaluate the relative role of various damping mechanisms. Both approaches suffer however from the same drawback, that the conditions of maximum wave damping are masked by cavity mode effects. In order to avoid this problem, we have to use additional (dimensionless) parameters for the description of the MC efficiency.

The first one is the so-called electron damping "figure of merit" Q_e, which is defined as the ratio of the total rf electromagnetic energy $W=1/(16\pi)\int(|\mathbf{E}|^2+|\mathbf{B}|^2)dx$, stored in plasma, to the total power $P_e=\int p_e\,dx$, absorbed by electrons, normalized to the wave frequency ω ("Total" means, that values are line-integrated along the plasma width in the radial direction):

$$Q_e = \omega \frac{W}{P_e}, \tag{10}$$

As shown in Sec. III, all power absorbed by electrons in present conditions, can be attributed to the mode-converted power, thus the Q_e-value can characterize the efficiency of the MC mechanism regardless of cavity-mode effects and competitive FW damping. When ion-cyclotron FW damping is weak, Q_e is equal, naturally, to the quality factor of the "global" plasma resonator.

The second parameter describes the relative role of the FW ion cyclotron damping in the MC electron heating scenario. It is defined as the ratio of total power , absorbed by electrons, to the total power, absorbed by all plasma species

$$P = \frac{P_e}{(P_e + P_i)} . \tag{11}$$

Another parameter is used to characterize the reflection rate of the incident FW at the MC region. Analogous with the transmission line theory, in 1D approach the concept of the traveling FW ratio can be introduced for the plasma region lying on the LFS of the MC layer. The parameter is defined as the ratio of the minimum and maximum values of the "poloidal" electric field amplitudes, determined in the LFS region between the boundary $R=n_{||}^2$ cut-off layer and the zone of strong absorption (see Fig.2(d)) :

$$G = \frac{\left|E_y^{min}\right|}{\left|E_y^{max}\right|}. \tag{12}$$

The value of $|E_y^{min}|$ and the difference $|E_y^{max}|-|E_y^{min}|$ represents respectively the traveling wave and the standing wave fraction of the LFS field pattern. So, the parameter will have a maximum G=1, when the whole incident rf power is absorbed at

the MC layer without LFS reflections and the traveling wave solely represents the LFS field pattern ($|E_y^{max}|=|E_y^{min}|$). On the contrary, the ratio will be minimized ($G\rightarrow 0$) in the case of negligible power absorption, when the FW undergoes multiple reflections in the LFS region. It is clear also, that correct calculation of the parameter G requires weak direct FW damping on its way to the plasma center and the FW perpendicular wavelength should be short enough compared with the plasma minor radius.

Together with the traveling FW ratio G, a reflection coefficient could be defined for a bounded plasma as $r=(|E_y^{max}|-|E_y^{min}|)/(|E_y^{max}|+|E_y^{min}|)$, although it does not carry any additional information, as compared to G. More expedient is to determine the average E_y field amplitude in the LFS region (the "falling" FW amplitude):

$$\left|E_y^f\right| = \frac{\left|E_y^{max}\right| + \left|E_y^{min}\right|}{2} \tag{13}$$

and to use it for normalization of the "poloidal" electric field value at the MC layer $|E_y^{mc}|$. Indeed, the ratio $|E_y^{mc}|/|E_y^f|$ is a very convenient parameter for estimating the role of $|E_y^{mc}|$ in the MC scheme, because it is not sensitive to the cavity mode effects. At the same time, this ratio can characterize the effect of the FW amplitude attenuation in the internal evanescent layer as well as it can be a criterion of MC layer location relative to the standing wave $|E_y|$ pattern. Obviously, it can be expected that for conditions of wide evanescent zone (strong local E_y attenuation), this ratio should always be much less than unity, and for the small Δ (low η) the ratio will strongly depend on MC layer position, reaching the maximum value of 2, when the MC layer is located at the $|E_y|$ pattern antinode.

Finally, the tunneling parameter $\eta=k_{\perp\infty}\Delta$ should also be redefined somehow in a global wave analysis, because the concept of asymptotic perpendicular wave number $k_{\perp\infty}$ is not fully consistent in a bounded plasma. In present studies instead of $k_{\perp\infty}$, defined in terms of the local values of the cold plasma tensor elements, estimated at the resonance point (see Eqn.(3)) , we used $<k_\perp>$ - the averaged FW perpendicular wavenumber. It is calculated using the hot plasma dispersion relation and averaged over the whole plasma region lying between the boundary cut-offs. It is worth saying that the difference between $<k_\perp>$ and $k_{\perp\infty}$ values was not too large for the present plasma parameters.

C. Mode conversion efficiency in a bounded plasma

The global field pattern treatment shows that the MC efficiency in a bounded plasma should strongly depend both on the MC layer position relative to the pattern and on the tunneling parameter. "VICE" computer simulations of the behavior of characteristic MC parameters, defined in previous subsection, were used to study these phenomena.

The role of MC layer location can be seen most clearly in conditions of fixed $\eta\equiv\eta_{cr}$ (see Fig.4). Analogous with simulations of Fig.2, the frequency variation in the range of 50-60 MHz was used to scan the MC layer along the minor radius in the central plasma regions. As can be seen on Fig.4(a), the value of $|E_y^{mc}|$ follows the global pattern during the scan and the local field attenuation due to the internal FW evanescence is not very strong: $|E_y^{mc}|/|E_y^{f}| \geq 1$ at maximum. When the MC layer

coincides with the pattern antinode and $|E_y^{mc}|$ has the highest values, the traveling FW ratio G in the LFS regions tends to unity, which means that there is no power flux, returning from the MC layer to the antenna (note that the notion of "single-pass absorption" is not strictly correct here, because the wave can still be reflected from the HFS cut-off). Simultaneously, the electron damping reaches the maximum (the lowest values of Q_e) and nearly 100% of injected power is absorbed by electrons. The last observation shows also, that in optimal conditions the role of competitive ion cyclotron FW damping is negligible. On the contrary, when the $|E_y^{mc}|$ value is minimal (the MC layer coincides with the global node), the traveling wave ratio G in the LFS region is close to zero and the electron power deposition is very weak. In this situation, the total power absorbed by electrons is determined mainly by direct FW damping due to ELD and TTMP mechanisms; the corresponding Q_e^{fw} behavior, estimated analytically in accordance with Ref. 23, is shown on Fig.4(c) as dashed line. Naturally, the ion cyclotron heating predominates over the electron heating under such circumstances.

Results of similar simulations with varying MC layer position and fixed tunneling parameter $\eta>\eta_{cr}$ and $\eta<\eta_{cr}$ are shown respectively on Fig.5 and Fig.6. Both figures also demonstrate the importance of the MC layer location near the global field antinode, as the electron power deposition correlates with $|E_y^{mc}|$ value. In conditions of maximum $|E_y^{mc}|$, the MC mechanism is dominating, Q_e values remain quite small and the power fraction, absorbed by electrons, is about 80-90%. At the same time, some differences can be mentioned. Unlike the $\eta=\eta_{cr}$ case, the traveling wave ratio G

never approaches unity (Fig.5(b)), which means that the FW undergoes reflections in the LFS region even in conditions of maximum power absorption. The clear distinction between $\eta<\eta_{cr}$ and $\eta>\eta_{cr}$ regimes can be seen in the maximum achievable amplitudes of the "poloidal" electric field $|E_y^{mc}|$ at the MC layer (compare Fig.5(a) and Fig6(a)). For large tunneling factors, the $|E_y^{mc}|$ is attenuated due to the FW evanescence near the MC layer and $|E_y^{mc}|/|E_y^{f}| < 1$ regardless of the MC layer position.

An interesting feature of discussed simulations is that for each η the ratio of the power absorbed by electrons to the square of the $|E_y^{mc}|$ is constant (see *e.g.* Fig.6(b)), despite the strong variation of this values during the frequency scan (The only exception can be noticed for frequencies corresponding to the MC layer exactly located at the global field node, when the mode conversion is so weak that other electron damping mechanisms are prevailing). This observation, produced in full wave kinetic treatment, is in agreement with simple cold plasma prediction of Eqn.(5) and justifies our qualitative model of MC processes in a bounded plasma.

Another kind of "VICE" simulations was used to demonstrate the role of the tunneling parameter in MC scheme. The behavior of MC characteristics was studied during the central plasma density scan (note that η is smoothly rising with n_e) in conditions when the MC layer location matches to a given antinode of the global field pattern. The latter was achieved by accurate frequency matching near f=55 MHz for each value of η to fit the maximum MC conditions (The same procedure and the density scan was used in simulations discussed on Fig.3). The results of simulations are shown on Fig.7. It can be seen from Fig.7(a) that the amplitude of "poloidal"

electric field at the MC layer is quickly decreasing with the tunneling parameter growth, which is explained by increasing FW attenuation due to the internal evanescence. On the contrary, the $P_e/|E_y^{mc}|^2$ ratio (Fig.7(b)) is rising in accordance with Eqn.(5). These opposite tendencies are balanced at $\eta=\eta_{cr}$ when the traveling FW component in LFS regions is maximum (Fig.7(c)) and electron damping is the highest (Fig.7(d)). Thus, a conclusion can be made that in a bounded plasma the requirement of proper tunneling parameter choice for optimizing the MC efficiency remains valid and the value of this critical parameter $\eta=\eta_{cr}\cong 0.22$ is the same as in "classical" treatment of an isolated Budden pair.

D. Cavity modes in mode conversion scheme

Up to this point, we studied the problem of MC efficiency regardless of cavity modes formation in the global plasma resonator, while it is clear, that such phenomena can be of primary importance in practical realization of the MC scheme. The discussed peculiarities of the field pattern formation and FW damping during the mode conversion introduce some unusual features in the behavior of the cavity modes as compared with other damping mechanisms. The cavity mode build-up in presence of MC layer turns to be very sensitive to its position. This effect is especially pronounced in $\eta=\eta_{cr}$ conditions. As it was found previously, the situation occurs when the MC layer coincides with the global $|E_y|$ antinode and $G\cong 1$, which means that there are no wave reflections on the LFS plasma boundary. Obviously, the global cavity mode build-up is impossible under such conditions. Conversely, if $G\cong 0$ (the MC layer is placed near the global $|E_y|$ pattern node), multiple FW reflections at the plasma

boundaries take place, resulting in a possibility of high-Q_e cavity mode formation regardless of η values. Thus, the quality factor of the global resonator (see Eqn.(10)) will depend evidently on the MC layer position, relative to the $|E_y|$ pattern nodes and antinodes.

Cavity mode formation in conditions of $\eta=\eta_{cr}$ and with three different MC layer positions is shown using numerical calculations (Fig.8). Global field patterns, typical for three cases, are close to the radial $|E_y|$ distributions, given by Fig.2(a-c). Plasma minor radius scan is used for the global resonator matching, because this procedure affects strongly neither the tunneling factor nor the MC layer position. Cavity mode build-up takes place at slightly different values of the minor radius a_c in three discussed cases, that is why we use normalized a/a_c minor radius as an abscissa in Fig.8. It can be seen from Fig.8 and Fig.2, that the cavity resonance curve turns to be less sharp as the MC layer approaches the $|E_y|$ antinode, revealing no resonance build-up at f=55MHz.

Significant increase of absolute values of the wave fields in plasma (Fig. 8(b)) and, hence, the mode converted power (Fig.8(a)) during the global cavity mode build-up can enhance the efficiency of MC scheme and extend the range of appropriate tunneling parameters. Indeed, in large scale tokamaks with reasonable plasma densities the spectrum of the global resonator eigenmodes is rather dense and the separate cavity resonances overlap, providing their quality factors are not too large (the damping is not negligible). Thus, efficient regime with quasicontinuous cavity mode spectrum can be achieved in conditions of $\eta\geq\eta_{cr}$, when the local $|E_y^{mc}|/|E_y^f|$ value is not too small and the electron damping is high enough. Similar regimes with

$\eta \leq \eta_{cr}$ are less favorable, because the $P_e/|E_y^{mc}|^2$ ratio is decreasing with η (Note, that majority of MC experiments with LFS FW exitation[6,7,8] were performed in conditions of $\eta \geq \eta_{cr}$). It is worth mentioning also that, in smaller tokamak plasmas, individual cavity modes of the global resonator can be excited. The cavity mode tracking during the whole rf pulse was produced in mode conversion experiments with the monopole LFS antenna on TO-2 tokamak[38], resulting in a very efficient central electron heating. These observations confirm the concept of the global resonator and demonstrate the applicability of the MC electron heating scheme for low-$k_{\|}$ FW excitation by a monopole antenna.

E. Discussion

Our analysis of the mode conversion in a bounded plasma can be considered as a certain generalization of existing models of cut-off-resonance-cut-off triplet resonator[5,9,10], which also predicts the possibility of 100% mode conversion in conditions of $\eta=\eta_{cr}$. The phase matching by optimum $k_{\|}$ selection in this approach can be treated as an analogue of the requirement of the MC position coincidence with the antinode of the $|E_y|$ pattern. Nevertheless, some remarks should be made, concerning this apparent similarity, because the practical conclusions of these treatments are somewhat different. Contrary to the triplet model, we never rely on a particular FW parallel wavenumber choice. For a given value of η the only requirement for maximizing the MC efficiency is to maximize the $|E_y^{mc}|$ magnitude by locating the MC layer near the global $|E_y|$ pattern antinode. For experimental situation of practical

interest, it always can be done regardless of $k_{||}$, because the field pattern in the bounded plasma of a large scale tokamak is typically represented by a structure of closely spaced field nodes and antinodes. Moreover, as the field pattern configuration depends also on $k_{||}$, it can be expected, that optimal conditions will always be satisfied for some $k_{||}$ values of the antenna spectrum. Thus, the present analysis shows that the MC scheme applicability can apparently be extended to a wider range of excited FW parallel wavelengths and the monopole phasing of LFS antennas can be used for MC scheme implementation. Such scenario looks favorable for studying the effects of low-hybrid (LH) and ion Bernstein wave synergism[5], because high initial parallel phase velocity $v_{||}=\omega/k_{||}$ of the mode converted IBW will lead to its preferential interaction with LH accelerated electrons (This does not mean that in absence of fast electrons mode conversion with monopole antenna is inefficient: rapid $k_{||}$ evolution of IBW in real plasma configuration[15,16] lead to inevitable IBW damping on bulk particles even if the initial $v_{||}$ is high).

Finally, some remarks should be made concerning the relevance of discussed 1D model results to the real situation, characterized by 3D toroidal geometry. At least two considerations can be noted, which give evidence that the 1D approach mostly underestimates the MC efficiency for the LFS FW excitation. The first one is connected with the fact that the tunneling parameter is not constant along the MC layer. Thus, non-central plasma regions can appear to be transparent for the LFS excited fast waves even in the case of their strong central evanescence. This leads to a possibility for fast waves to skirt the central plasma regions, reflect at the HFS $R=n_{||}^2$ cut-off and undergo the mode conversion with HFS incidence. This phenomena can

significantly enhance MC efficiency, especially in $\eta > \eta_{cr}$ conditions. Such effects were observed during computer modeling activities with 2D full wave code "ALCYON"[39] (see also Ref. 40). Another 2D phenomenon, which can lead to notable increase of the mode converted power, as compared with the plain model, is the FW focusing in the central plasma regions due to volumetric effects. The role of this factor in explanation of strong on-axis electron heating, as well as a comparison of 1D and 2D code simulations was reported in Ref. 8.

Account of real tokamak magnetic configuration can also introduce some less favorable features into the MC electron heating scheme, predicting broader power deposition profiles and the possibility of enhanced ion heating. Ray-tracing calculations in 3D current-carrying plasma[15,16] show that IBW rays leaving the MC region can undergo complicated evolution, concerning both their trajectories and parallel wavenumbers. If initial IBW phase velocity is far from the local electron thermal velocity, the situation is possible when IBW is damped preferentially by ions, as the IBW trajectory goes close to an ion cyclotron resonance layer. Thus, the FW ion damping being small and the MC efficiency being high, the actual electron power deposition can be lower, comparing with 1D model predictions.

Generally, the 1D full wave treatment, reported here, along with its generalizing meaning, is valuable in a sense, that it provides solid guidelines for optimal experimental parameters definition and evaluate the capabilities of the MC electron heating scheme.

V. CONCLUSIONS

In this paper, we made an attempt to demonstrate a consistent one-dimensional picture of the mode conversion process at the ion-ion hybrid resonance in a bounded plasma of a tokamak, and to clarify the role of the global fast wave interference and cavity effects in determination of the MC efficiency. The concept of the "global resonator"[7], formed by $R=n_{||}^2$ boundary cut-offs, was justified and the important role of the tunneling factor η for the global field pattern formation and optimization of the MC efficiency[9,10] was confirmed.

Starting from simple considerations, based on the Budden equation analysis, which were strongly supported by 1D full wave kinetic simulations, we examined the peculiarities of MC scheme, based on the LFS fast wave launching. It was found, that the local value of the "poloidal" electric field $|E_y^{mc}|$ at the mode conversion layer is the parameter determining the general behavior of the involved processes. This value depends definitely on the MC layer position, relative to the global field pattern, while the pattern configuration is sensitive to the tunneling parameter η. Location of the MC layer on the global $|E_y|$ pattern antinode in conditions of $\eta=\eta_{cr}\cong 0.22$ results in a critical regime occurrence, where the MC efficiency is maximum and the field pattern in the LFS regions is represented solely by the FW, traveling from the antenna to the MC layer. MC layer location on the global field node leads to minimization of electron power deposition and purely standing wave pattern formation in the entire plasma volume. It is important that realization of the critical regime does not suppose any requirement of particular parallel wavenumber choice; thus present analysis demonstrates a wider range of the MC scheme applicability.

The role of ion cyclotron effect as a competitive FW damping mechanism was analyzed. It was found that the power equipartition strongly depends on the MC layer position relative to the global wave pattern. In regimes, close to critical, ion power deposition for the Tore Supra parameters is negligible, even in the situation, when the cyclotron layer crosses the central hot plasma regions.

The global resonator cavity modes were recognized as phenomena which can strongly enhance the MC efficiency, because their build-up cause significant growth of the $|E_y^{mc}|$ field amplitude at the MC layer. Certain peculiarities of the cavity effects were revealed, showing dependence of the global resonator quality factor on the MC layer position. Formation of the global cavity mode in critical regime was found impossible.

The discussed picture is consistent with basic results of well-known analytical models and explains some effects previously observed during numerical simulations.

ACKNOWLEDGMENTS

The authors are grateful to Dr. Yu. Petrov for fruitful discussions.

REFERENCES

[1] A. Bécoulet, Plasma Phys. Controlled Fusion **38**, A1(1996).

[2] R. Majeski, C. K. Phillips, and J. R. Wilson, Phys .Rev. Lett. **73**, 2204 (1994).

[3] N. Fisch, in *Proceedings of the 21st EPS Conference on Controlled Fusion and Plasma Physics,* Montpellier, 1994 (European Physical Society, Geneva, 1994), Vol. 18B, Part II, p. 6401.

[4] C. Gormezano, in *Proceedings of the 10th Topical Conference on RF Power in Plasmas,* Boston, 1993, AIP Conf. Proc. 289 (American Institute of Physics, New York, 1993), p. 87.

[5] A. K. Ram, A. Bers, V. Fuchs, and S. D. Schultz, in *Proceedings of the 21st EPS Conference on Controlled Fusion and Plasma Physics,* Montpellier, 1994 (European Physical Society, Geneva, 1994), Vol. 18B, Part III, p. 1134.

[6] R. Majeski, J. H. Rogers, S. H. Batha, A. Bers, R. Budny, D. Darrow, H. H. Duong, R. K. Fisher, C. B. Forest, E. Fredrickson, B. Grek, K. Hill, J. C. Hosea, D. Ignat, B. LeBlanc, F. Levinton, S. S. Medley, M. Murakami, M. P. Petrov, C. K. Phillips, A. Ram, A. T. Ramsey, G. Schilling, G. Taylor, J. R. Wilson, and M. C. Zarnstorff, Phys. Plasmas **3**, 2006 (1996).

[7] B. Saoutic, A. Bécoulet, T. Hutter, D. Fraboulet, A. K. Ram and A. Bers, Phys. Rev. Lett. **76**, 1647 (1996).

[8] P. T. Bonoli, P. O'Shea, M.Brambilla, S. N. Golovato, A. E. Hubbard, M. Porkolab, Y. Takase, R. L. Boivin, F. Bombarda, C. Christiansen, C. L. Fiore, D. Garnier, J. Goetz, R. Granetz, M. Greenwald, S. F. Horne, I. H. Hutchinson, J. Irby, D. Jablonski, B. LaBombard, B. Lipschltz, E. Marmar, M. May, A. Mazurenko, G. McCracken, R. Nachtrieb, A. Niemczewski, H. Ohkawa, D. A. Pappas, J.Reardon, J. Rice, C. Rost, J. Schachter, J. A. Snipes, P. Stek, K. Takase, J. Terry, Y. Wang, R. L. Watterson, B. Welch, and S. M. Wolfe, Phys. Plasmas **4**, 1774 (1997).

[9] V. Fuchs, A. K. Ram, S. D. Schultz, A. Bers, and C. N. Lashmore-Davies, Phys. Plasmas **2**, 1637 (1995).

[10] A. K. Ram, A. Bers, S. D. Schultz, and V. Fuchs, Phys. Plasmas **3**, 1976 (1996).

[11] C. N. Lashmore-Davies, V. Fuchs, A. K. Ram, and A. Bers, Phys. Plasmas **4**, 2031 (1997).

[12] K. G. Budden, *Radio Waves in the Ionosphere* (Cambridge University Press, Cambridge, 1961).

[13] T. H. Stix, *Theory of Plasma Waves* (McGraw-Hill, New-York, 1962).

[14] In Ref. 11 the mode was identified as the ion hybrid wave, the only branch of the IBW family, which can propagate at frequencies between the cyclotron frequencies of the plasma ion species.

[15] A. K. Ram and A. Bers, Phys. Fluids B **3**, 1059 (1991).

[16] Yu. V. Petrov, Nucl. Fusion **34**, 63 (1994).

[17] D. J. Swanson, Phys. Rev. Lett. **36**, 316 (1976).

[18] F. W. Perkins, Nucl. Fusion **17**, 1197 (1977).

[19] J. Jacquinot, B. D. McVey, and J. E. Scharer, Phys. Rev. Lett. **39**, 88 (1977).

[20] J. A. Heikkinen, T. Hellsten, and M. J. Alava, Nucl. Fusion **31**, 417 (1991).

[21] T. H. Stix and D. G. Swanson, in *Handbook of Plasma Physics*, edited by A. Galeev and R. N. Sudan (North-Holland, Amsterdam, 1983), Vol. 1, p. 335.

[22] Equipe TFR, in *Plasma Physics and Controlled Nuclear Fusion Research,* Proceedings of the 9th International Conference, Baltimore, 1982 (International Atomic Energy Agency, Vienna, 1983), Vol. 2, p. 17.

[23] T. H. Stix, Nucl. Fusion **15**, 737 (1975).

[24] C. F. F. Karney, F. W. Perkins, and Y-C. Sun, Phys. Rev. Lett. **42**, 1621 (1979).

[25] Y. C. Ngan and D. G. Swanson, Phys. Fluids **20**, 1920 (1977).

[26] P. L. Colestock and R. J. Kashuba, Nucl. Fusion **23**, 763 (1983).

[27] A. Fukuyama, S. Nishiyama, K. Itoh, and S-I. Itoh, Nucl. Fusion **23**, 1005 (1983).

[28] O.Sauter, L. Villard, and X. Llobet, in *Proceedings of the 14th EPS Conference on Controlled Fusion and Plasma Physics,* Madrid, 1987 (European Physical Society, Geneva, 1987), Vol. 11D, Part III, p. 957.

[29] E. F. Jaeger, D. B. Batchelor, and H. Weitzner, Nucl. Fusion **28**, 53 (1988).

[30] M. Brambilla, Plasma Phys. Controlled Fusion **31**, 723 (1989).

[31] D. Van Eester and R. Koch, Phys. Lett. A **227**, 97 (1997).

[32] D. Fraboulet, A. Bécoulet and G. Pelletier , in *Proceedings of the 12th Topical Conference on RF Power in Plasmas,* Savannah, 1997, AIP Conf. Proc. 403 (American Institute of Physics, New York, 1997), p. 363.

[33] D. Fraboulet, Ph. D. thesis, Universite J. Fourier, Grenoble I, 1996.

[34] D. J. Gambier and A. Samain, Nucl. Fusion **25**, 283 (1985).

[35] A. Bécoulet, D. Fraboulet, G. Giruzzi, D. Moreau, B. Saoutic, and J. Chinardet, Phys. Plasmas **1**, 2908 (1994).

[36] Equipe Tore Supra, in *Fusion Energy,* Proceedings of the 16th International Conference, Montreal, 1996 (International Atomic Energy Agency, Vienna, 1997), Vol. 1, p. 141.

[37] The fast wave phase shift in the internal evanescence layer is negligible for $\eta<1$ (e.g. see considerations of Ref. 10).

[38] I. A. Kovan, P. E. Kovrov, and I. A. Monakhov, in *Proceedings of the 17th EPS Conference on Controlled Fusion and Plasma Heating,* Amsterdam, 1990 (European Physical Society, Geneva, 1990), Vol. 14B, Part III, p. 991.

[39] Yu. V. Petrov and A. Bécoulet, "Approach to coupling of full-wave codes with ray tracing codes", submitted to Computer Phys. Communications.

[40] A. Jaun, T. Hellsten, and S. C. Chiu, Nucl. Fusion **38**, 153 (1998).

FIGURE CAPTIONS:

Fig. 1 Typical radial behavior of (a) the perpendicular wavenumber, given by the "hot plasma" dispersion relation and (b) the parallel electric field amplitude, (c) the amplitude of the perpendicular left-hand polarized electric field, (d) the density of power, absorbed by the plasma species, (e) the radial Pointing flux, given by "VICE" simulations.

Fig. 2 Radial behavior of the "poloidal" electric field amplitude for $\eta \cong \eta_{cr}$ ($n_e(0)=4\times10^{19}$ m^{-3}) and different locations of the mode-conversion layer (dashed line) relative to the field pattern.

Fig. 3 Radial behavior of the "poloidal" electric field amplitude for different values of the tunneling parameter. The frequency is matched near f=55MHz to fit the maximum mode-conversion conditions for each value of η. The tunneling parameter is controlled by the plasma density $n_e(0)$ adjustment: (a) 3×10^{19} m^{-3}, (b) 4×10^{19} m^{-3}, (c) 6×10^{19} m^{-3}, (d) 10×10^{19} m^{-3}, (e) 20×10^{19} m^{-3}. The location of the MC layer is shown by the dashed line.

Fig. 4 Behavior of specific MC characteristics (see Eqs.(10), (11), (12) and (13)) during the MC layer position scanning by the frequency variation for the case of $\eta \equiv \eta_{cr}$ ($n_e(0)=4\times10^{19}$ m^{-3}) : (a) the squared ratio of amplitudes of E_y field at the mode-conversion layer and E_y field of the "falling" fast wave, (b) the traveling wave ratio in the LFS region, (c) the electron damping "figure of merit", (d) the fraction of the power, absorbed by electrons. Dashed line represents an analytical estimate[23] of Q_e^{fw}, taking into account only direct fast wave damping due to ELD and TTMP mechanisms.

Fig. 5 Behavior of specific MC characteristics (see caption of Fig.4) during the MC layer position scanning by the frequency variation for the case of $\eta=0.4$ ($n_e(0)=6\times10^{19}m^{-3}$).

Fig. 6 Behavior of specific MC characteristics (see Eqs.(10), (11), and (13)) during the MC layer position scanning by the frequency variation for the case of $\eta=0.1$ ($n_e(0)=3\times10^{19}$ m^{-3}) : (a) the squared ratio of amplitudes of E_y field at the mode-conversion layer and E_y field of the "falling" fast wave, (b) the ratio of the power, absorbed by electrons to the square of "poloidal" electric field at the MC layer, (c) the electron damping "figure of merit", (d) the fraction of the power, absorbed by electrons. Dashed line on Fig.6(c) represents an analytical estimate[23] of Q_e^{fw}, taking into account only direct fast wave damping due to ELD and TTMP mechanisms.

Fig. 7 Dependence of specific MC characteristics (see Eqs.(10), (11), (12) and (13)) on the tunneling factor; the frequency is matched near f=55MHz for each value of η to fit the conditions of maximum mode-conversion (i.e. maximize $|E_y^{mc}|$): (a) the squared ratio of amplitudes of E_y field at the mode-conversion layer and E_y field of the "falling" fast wave, (b) the ratio of the power, absorbed by electrons, to the square of E_y amplitude at the MC layer (normalized to unity at $\eta=\eta_{cr}$); solid line - full wave "VICE" calculations, dashed line - cold plasma estimate with Eqn.(5), (c) the traveling wave ratio in the LFS region, (d) the electron damping "figure of merit".

Fig. 8 Cavity mode formation during the plasma minor radius variation for conditions of $\eta \equiv \eta_{cr}$ ($n_e(0)=4\times10^{19}$ m^{-3}) and different positions of the mode-conversion layer relative to the E_y field pattern: (a) the total power, absorbed by electrons, (b) the total rf electromagnetic energy, stored in plasma. The dashed, dotted and solid curve roughly corresponds to the field patterns, shown respectively on Fig.2 (a), (b) and (c). The minor radius is normalized to the value a_c , when the mode build-up takes place.

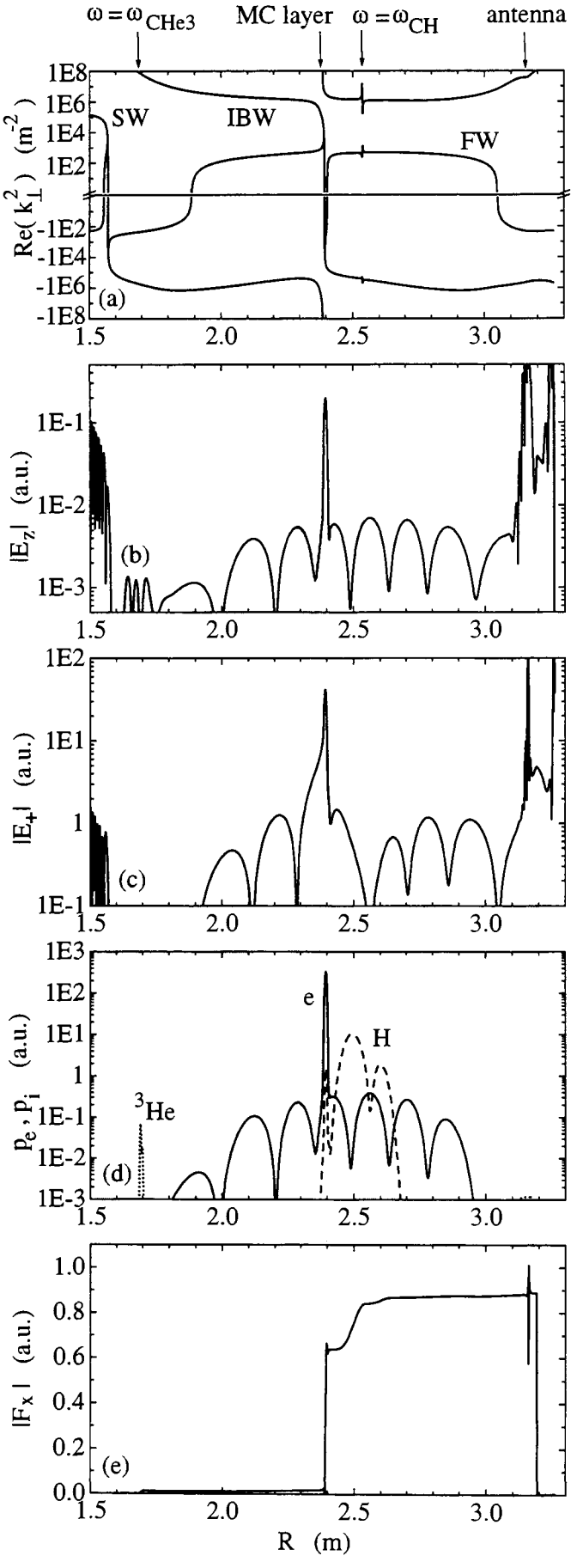

"original" Figure 1 Monakhov *et al.*

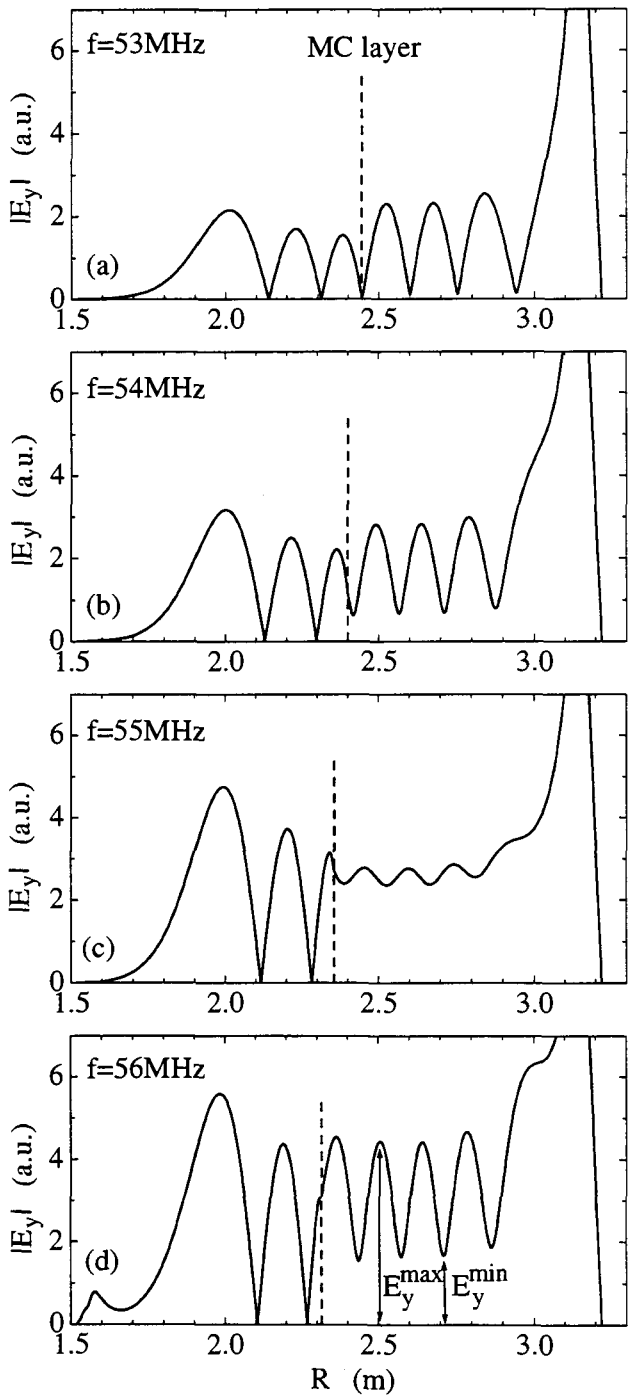

"original" Figure 2 Monakhov *et al.*

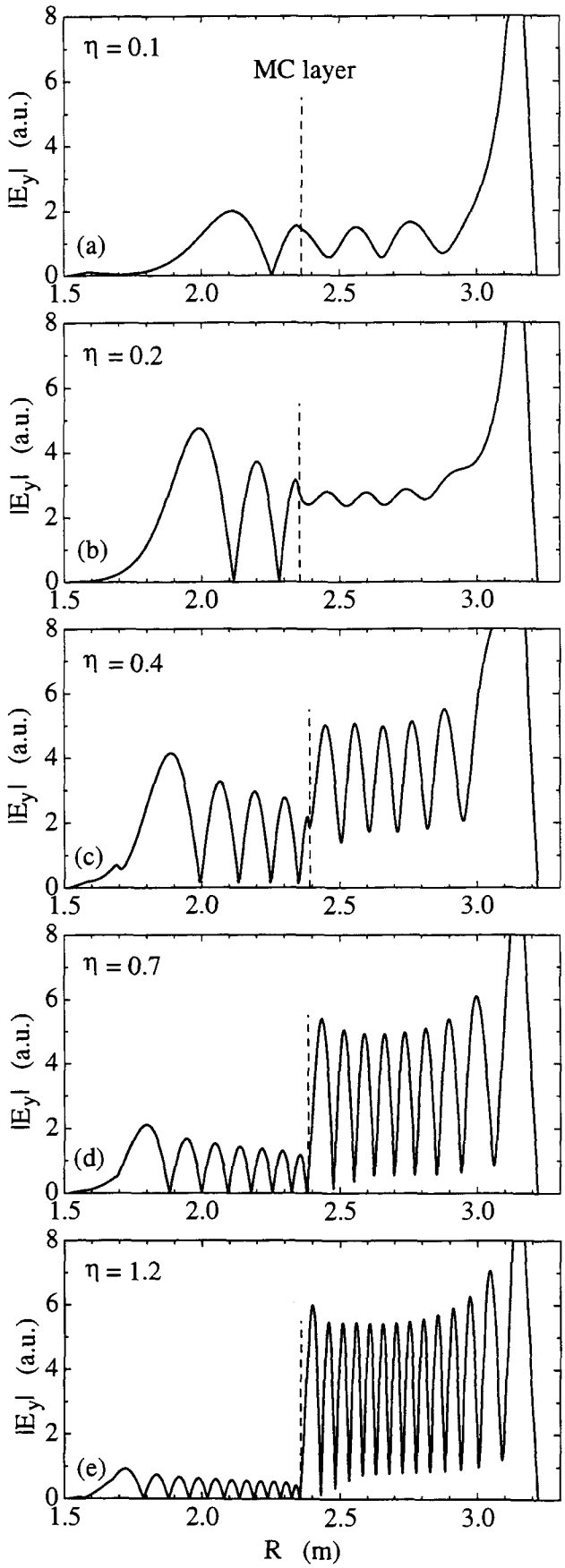

"original" Figure 3 Monakhov *et al.*

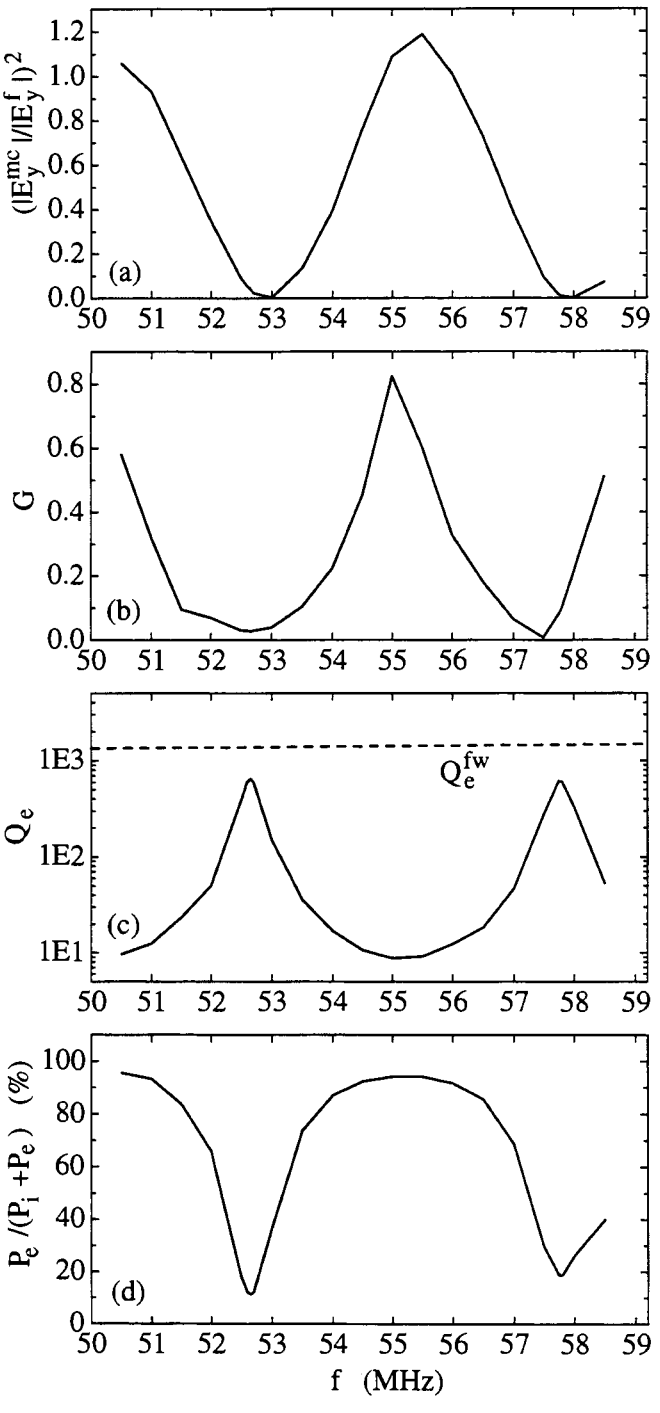

"original" Figure 4 Monakhov *et al.*

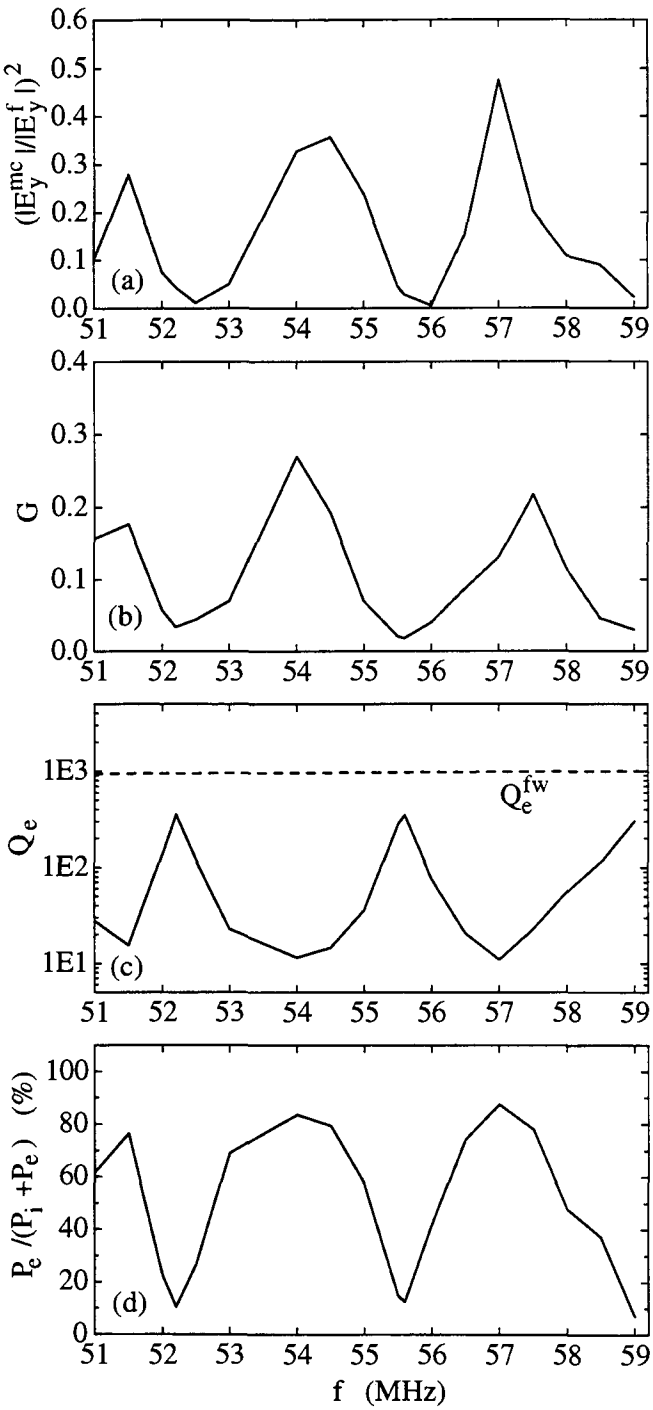

"original" Figure 5 Monakhov *et al.*

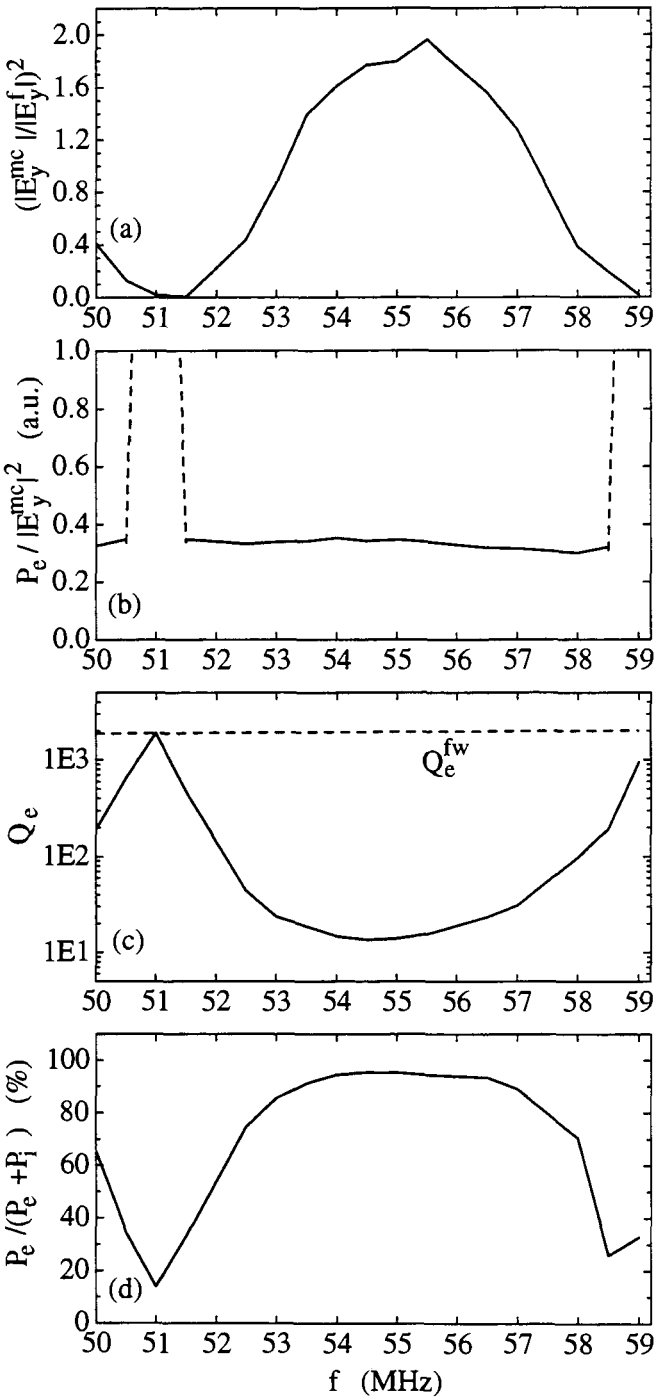

"original" Figure 6 Monakhov *et al.*

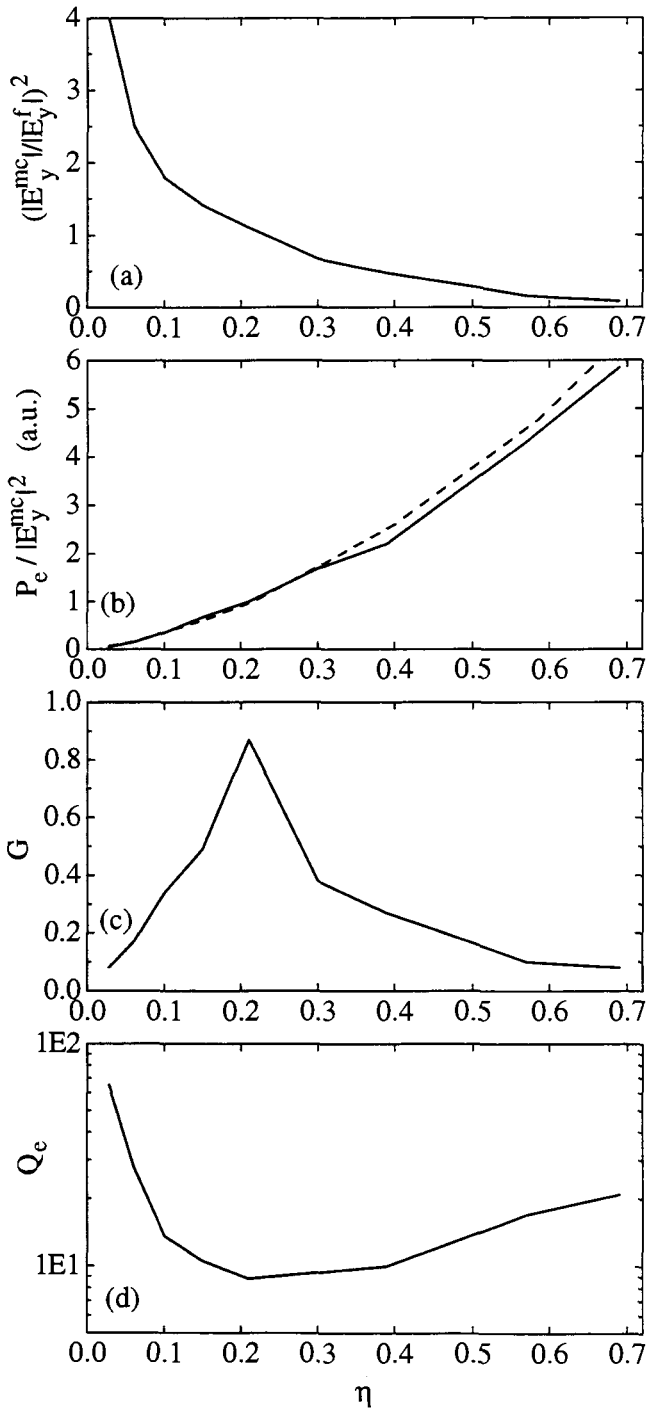

"original" Figure 7 Monakhov *et al.*

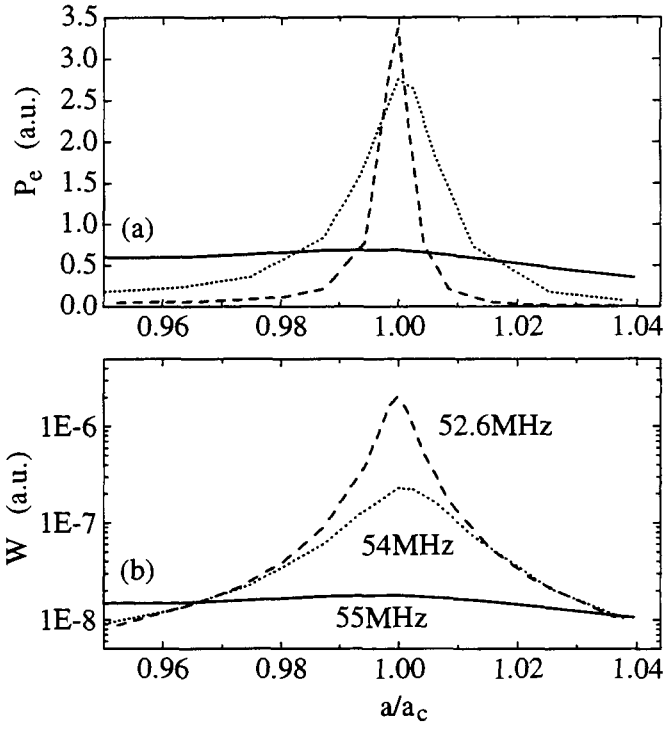

"original" Figure 8 Monakhov *et al.*